PROMPT ESTIMATION OF STRONG GROUND MOTION NEAR FOCAL REGION BASED ON FAULT INVERSION FROM ACCELERATION RECORDS

Masumitsu KUSE[1], Masata SUGITO[2] and Nobuoto NOJIMA[3]

[1] *Assistant Professor, River Basin Research Center, Gifu University, Gifu City, Japan*
[2] *Professor, River Basin Research Center, Gifu University, Gifu City, Japan*
[3] *Professor, Department of Civil Engineering, Gifu University, Gifu City, Japan*
Email: kuse@gifu-u.ac.jp, sugito@gifu-u.ac.jp, nojima@gifu-u.ac.jp

ABSTRACT :

The inversion technique on the basis of acceleration envelope fitting is applied for two recent inland earthquakes. One is the Noto Hanto Earthquake in 2007 (M=6.9) and the other is the Niigataken Chuetsu-oki Earthquake (M=6.8). The base-rock strong motion records obtained by K-NET and KiK-net observation systems are converted to those for engineering base-rock level with the shear wave velocity of V_s=500-600 m/sec. These acceleration time histories are used for the inversion of faults focusing on the asperity distribution on the assumed fault location. Next, on the basis of the estimated fault models including the asperity distribution, the strong ground motions are simulated at all over the areas around the faults. The characteristic of the distribution of the JMA (Japan Meteorological Agency) seismic intensity is compared with that from the observed strong motion records. The degree of dependence of the seismic intensity distribution on the asperity distribution is discussed in the comparison for the case of intermediate and relatively large fault events.

KEYWORDS: Prompt estimation of strong ground motion, The Noto Hanto Earthquake in 2007, The Niigataken Chuetsu-oki Earthquake in 2007, Asperity

1. INTRODUCTION

In 2007, two typical inland-shallow earthquakes occurred in Ishikawa and Niigata prefectures, central-north part of Japan. One is The Noto Hanto Earthquake in 2007 (M=6.9), and the other is The Niigataken Chuetsu-oki Earthquake in 2007 (M=6.8). In these earthquake, many strong motion records were obtained by K-NET(2007) and KiK-net(2007), which are the observation network operated by National Research Institute for Earth Science and Disaster Prevention.

In this study, the asperity pattern is represented by the normalized coefficient for the superposition of the evolutionary power spectra assigned for each sub-event in the EMPR (Sugito *et al*., 2000). EMPR can simulate nonstationary strong motion for given fault parameters including asperity distribution. Data used for inversion are acceleration envelopes calculated using acceleration records from KiK-net database. The inversion technique developed by Kuse *et al*. (2004a, 2004b), estimates the asperity distribution by use of the envelope of acceleration time history. In the following, the inversion technique used for this study is outlined, and its application to estimation of the source process in these earthquakes, are presented.

2. OUTLINE OF SOURCE PROCESSS INVERSION

2.1. Outline of Source Process Inversion

Figure 1 shows the flow of the inversion method by Kuse et al. (2004b). In the analysis, the location of hypocenter (latitude, longitude, depth) and the fault parameters (length, width, strike, dip angle) are dealt with

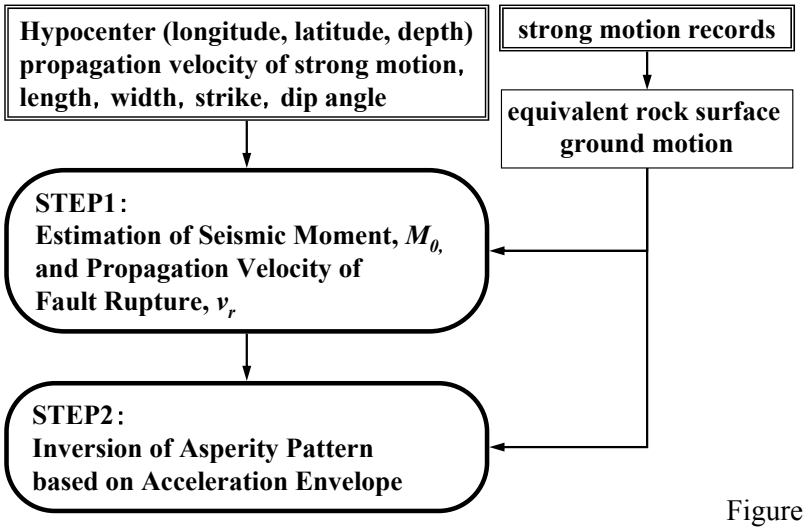

Figure 1 Outline for Inversion of Source Process

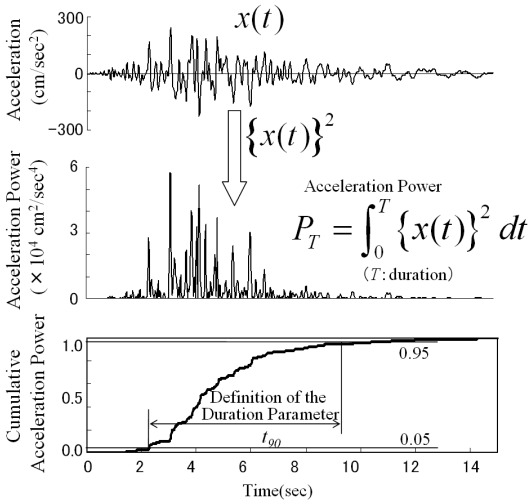

Figure 2 Definition of Duration Parameter t_{90} with Acceleration Total Power P_T

as the given parameters. The inversion method consists of two steps: STEP 1 for estimation of the seismic moment and the propagation velocity of fault rupture and STEP 2 for inversion of asperity pattern.

In STEP 1, the seismic moment, M_0, and the propagation velocity of rupture, v_r, are identified. The details are described in Kuse *et al*. (2000). At this stage the asperity distribution on the fault plane is not considered. The two ground motion parameters are used for the inversion of M_0 and v_r; one is the acceleration total power, P_t, and the other, the strong motion duration, t_{90}. The definition of P_t and t_{90} are shown in Figure 2. The acceleration total power, P_t, defined by Eq. 2.1 represents the square sum of acceleration time history over the total record length T:

$$P_t = \int_0^T \{x(t)\}^2 dt \qquad (2.1)$$

where, P_t is the acceleration total power (cm^2/sec^3), $x(t)$ is the acceleration (cm/sec^2) at time t, T is the total record length of the accelerogram (sec). The parameter, t_{90}, represents the duration defined as the time length between 5% and 95 % in terms of the accumulation of acceleration power as shown in Figure 2.

Next, in the STEP 2, the inversion of normalized ratio of released acceleration power on the fault plane is performed using the seismic moment, M_0, and the propagation velocity of rupture, v_r, obtained in STEP1. Kuse *et al*. (2004a, 2004b) proposed two alternative ways of processing acceleration time histories; one deals with the envelope of acceleration time history, and the other deals with the envelope of bandpass-filtered acceleration time history for low, middle, and high frequency ranges. In this paper, the envelope of acceleration time history for the estimation of asperity pattern was employed.

2.3. Conversion of the Strong Motion Records on the Rock Surface

In this study, the dataset of strong motion records that were observed by KiK-net (2007) stations, were used. Generally two seismometer both on ground surface and underground base rock level are set in the KiK-net system. The inversion method used here is based on the strong motion prediction model, EMPR (Earthquake Motion Prediction model on Rock surface) (Sugito *et al*., 2000). The EMPR that was used for the analysis is the strong motion prediction model on the rock surface that was defined as the shear wave velocity of 400-600m/sec. Therefore, as shown Figure 1, these records were converted to those on the rock surface level with the shear wave velocity of approximately 400-600m/sec.

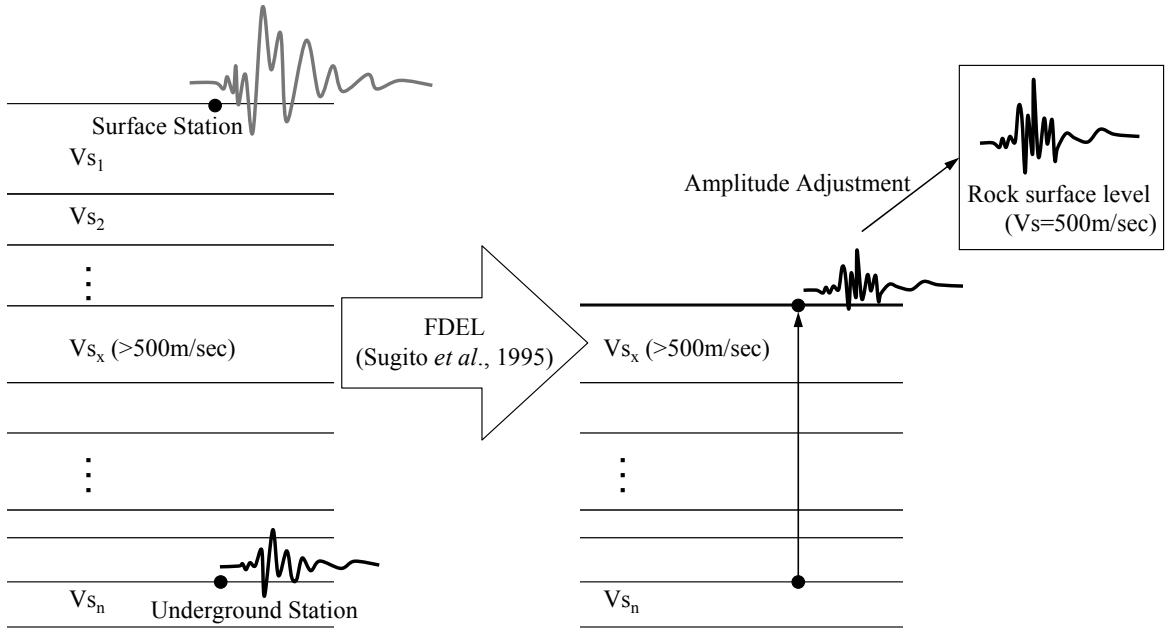

Figure 3 Schematic Diagram for Calculation of Rock Surface Ground Motion with Shear wave Velocity of V_s=500 m/sec

Figure 3 shows the outline of conversion for the strong motion records. First, the record on rock surface level (over 500m/sec) was converted based on the soil profile models for these observation stations. The response analysis of layered ground, using the program code FDEL (Frequency Dependent Equi-Linearized technique) (Sugito *et al*., 1995), has been applied. In this analysis, the lower limits of damping h_{min} for the rock and harder layer (over 500m/sec) was fixed as h_{min}=2.5% based on Enomoto *et al*. (2007). In case of other soils (clay, silt, sand, gravel), the lower limit was fixed as h_{min}= 5%.

Next, the free-rock surface ground motions were converted to those for the shear wave velocity of 500m/sec based on Midorikawa (1987). The amplification of earthquake motion from the seismic bedrock (Vs=3,000m/sec) to the surface is represented in the following equation.

$$\begin{aligned} A_v &= 170\, V_s'^{-0.6} \quad (V_s' < 1{,}100 \ \text{m/sec}) \\ &= 2.5 \quad (V_s' \geq 1{,}100 \ \text{m/sec}) \end{aligned} \tag{2.2}$$

where, A_v is the amplitude ratio of maximum velocity from the seismic bedrock to the surface, V_s' is the average of shear wave velocity at 30m below the surface of ground (m/sec).

The correction factor, A, of acceleration time history from rock surface level of V_s=V_{sx} to $V_s = 500$ m/sec is given in the following.

$$A = \frac{A_v(500)}{A_v(V_{sx})} \tag{2.3}$$

where, A is the correction factor of the earthquake motion, $A_v(500)$, $A_v(V_{sx})$ are the amplitude given Eq. 2.2, V_{sx} is the shear wave velocity on the rock surface at each individual KiK-net site (See Figure 3).

3. APPLICATION TO THE SEVERAL EARTHQUAKES

3.1. The Noto Hanto Earthquake in 2007

The inversion method presented above was applied to the Noto Hanto Earthquake in 2007. The dataset of strong motion records obtained during this earthquake was used. Figure 4 shows locations of the fault and the strong motion stations of KiK-net (2007) around focal region. The records used in the analysis were obtained at the stations represented by blue circled numbers in Figure 4. The projection of the fault plane on the ground surface is also given in Figure 4. As shown Table 3.1(a), the 22 horizontal components of acceleration records obtained at the 11 stations were used in the analysis. The strong motion records were selected according to the following conditions; the peak acceleration at surface ground is larger than 100m/sec^2, or the records obtained in

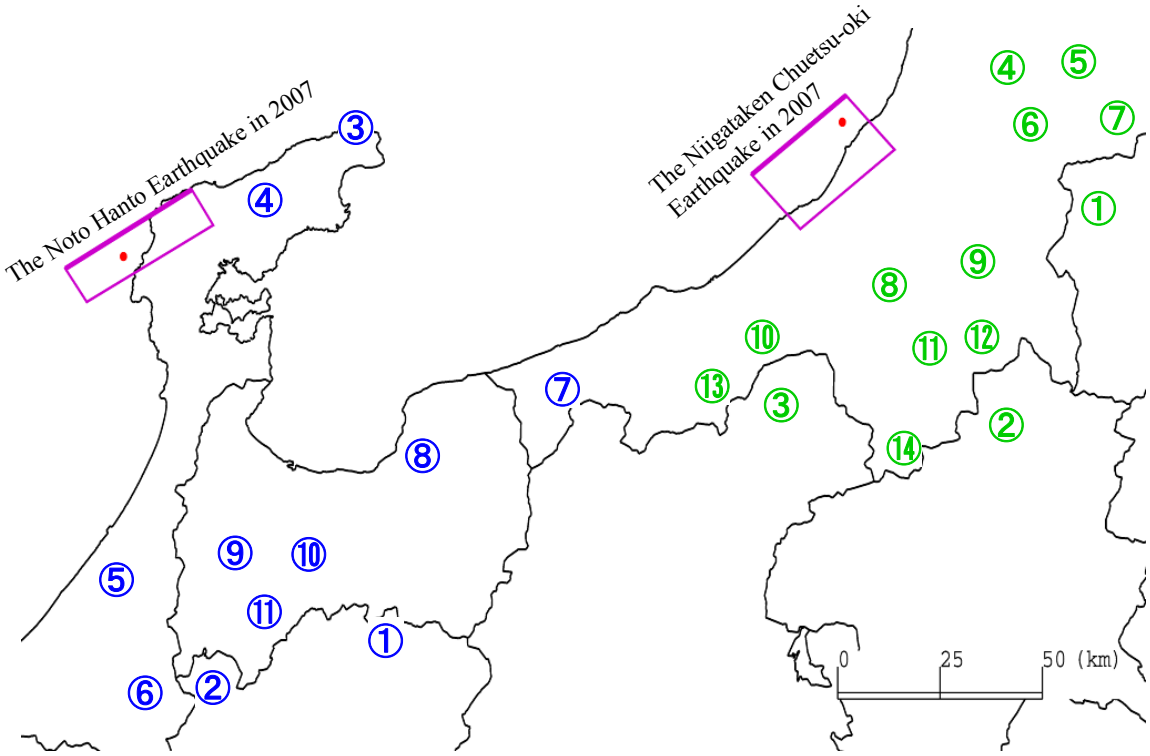

Figure 4 Location of Strong Motion Stations and Two Faults
(Red circle represents epicenter, blue and green circled number represents location of observation stations. The strong motion records at blue circled number are used for The Noto Hanto Earthquake in 2007, and those at green circled number for The Niigataken Chuetsu-oki Earthquake in 2007.)

Table 3.1 List of Strong Motion Records

(a) The Noto Hanto Earthquake in 2007

No.	Station Code	Maximum Acceleration on Soil Surfece (cm/sec^2)		Maximum Acceleration on Rock Surfece (Vs=500m/sec) (cm/sec^2)		Epicentral Distance (km)
		EW	NS	EW	NS	
①	GIFH10	81.40	-93.68	-44.90	-37.90	115.4
②	GIFH13	-77.09	102.00	-32.10	-28.80	109.6
③	ISKH01	-120.96	-360.24	45.90	76.50	64.5
④	ISKH02	369.49	258.62	-263.90	-461.80	37.3
⑤	ISKH07	57.06	-96.75	18.90	-21.70	80.6
⑥	ISKH09	184.59	179.85	67.50	67.20	108.4
⑦	NIGH16	-49.04	-59.55	-51.40	39.00	111.5
⑧	TYMH04	38.83	-38.27	-36.50	35.00	88.2
⑨	TYMH05	96.39	-113.05	37.00	-52.20	79.0
⑩	TYMH06	86.45	65.74	-30.80	-29.10	87.1
⑪	TYMH07	-82.03	-58.90	-46.50	-23.70	95.4

(b) The Niigataken Chuetsu-oki Earthquake in 2007

No.	Station Code	Maximum Acceleration on Soil Surfece (cm/sec^2)		Maximum Acceleration on Rock Surfece (Vs=500m/sec) (cm/sec^2)		Epicentral Distance (km)
		EW	NS	EW	NS	
①	FKSH21	-100.72	83.42	30.5	-22.1	66.1
②	GNMH13	-72.48	104.62	-13.8	19.7	85.4
③	NGNH29	101.44	101.16	-40.8	40.1	71.6
④	NIGH06	-148.38	-149.20	-42.3	-52.5	42.3
⑤	NIGH07	-66.59	-72.38	27.8	-23.8	59.1
⑥	NIGH09	-123.47	121.83	39.5	63.4	45.7
⑦	NIGH10	64.65	91.72	-28.9	-26.9	66.6
⑧	NIGH11	124.11	161.31	78.5	92.1	42.5
⑨	NIGH12	-187.94	109.05	49.2	48.3	48.2
⑩	NIGH13	-165.90	261.25	118.3	-160.7	57.1
⑪	NIGH14	-84.23	-90.00	35.1	-40.7	60.6
⑫	NIGH15	42.36	46.34	-31.5	20.3	64.0
⑬	NIGH18	-95.87	-94.96	-36.6	-44.6	73.3
⑭	NIGH19	-47.57	-131.13	-29.6	-64.4	82.5

near-field region. As previously mentioned, these records were converted to those on rock surface level with the shear wave velocity of 500m/sec.

Table 3.2 shows the fault parameters including the estimated parameters, M_0, and v_r, through STEP 1. Figure 5(a) shows the asperity pattern that has been obtained by the STEP 2. For the comparison, Figure 5(b) shows the distribution of coseismic slip estimated by Aoi and Sekiguchi. (2007). The location of asperity for these analysis are consistent.

Table 3.2 Fault Parameters

Fault Parameter		The Noto Hanto Earthquake in 2007	The Niigataken Chuetsu-oki Earthquake in 2007
Hypocenter	Latitude (degree)	37.24	37.54
	Longitude (degree)	136.65	138.61
	Depth (km)	11.0	8.0
Fault Plane (after Aoi et al., 2007)	Length (km)	36.0	30.0
	Width (km)	24.0	24.0
	Strike (degree)	58.0	49.0
	Dip Angle (degree)	66.0	42.0
*Seismic Moment M_0 (Nm)		4.35×10^{18}	1.83×10^{18}
*Propagation Velocity of Fault Rupture v_r (km/sec)		1.89	1.89

(*Estimated in STEP 1)

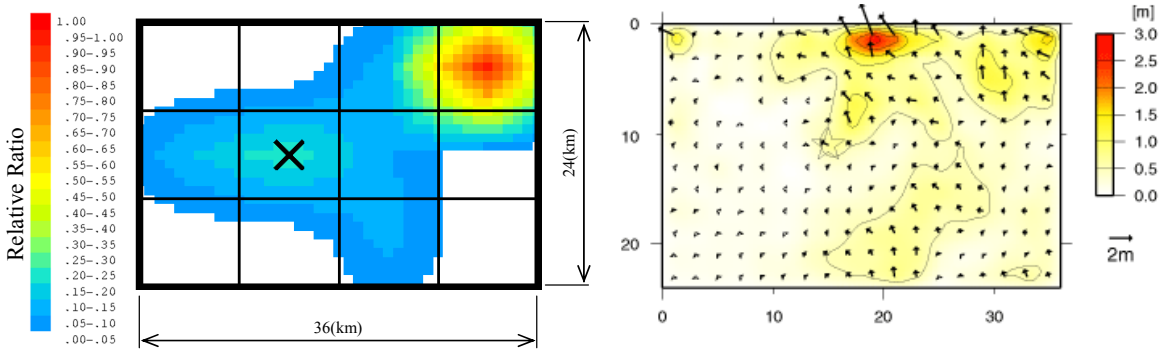

(a) Asperity Pattern (This Study) (b) Distribution of Fault Slip (Aoi and Sekiguthi, 2007)

Figure 5 Distribution of Asperity (The Noto Hanto Earthquake in 2007)

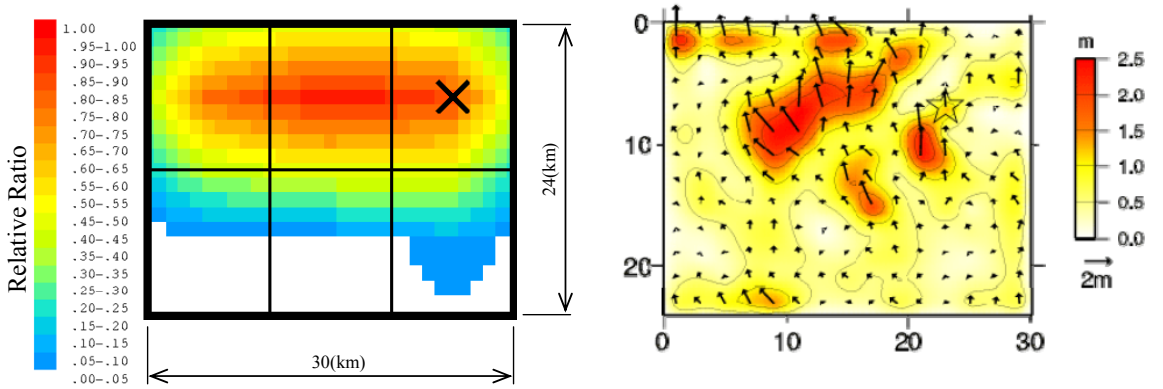

(a) Asperity Pattern (This Study) (b) Distribution of Fault Slip (Aoi *et al.*, 2007)

Figure 6 Distribution of Asperity (The Niigataken Chuetsu-oki Earthquake in 2007)

3.2. The Niigataken Chuetsu-oki Earthquake in 2007

In the same procedure the inversion technique was applied to the Niigataken Chuetsu-oki Earthquake in 2007. Figure 4 shows locations of the fault model and the strong motion stations of KiK-net(2007) around focal region. As shown table 3.1(b), the 28 horizontal acceleration records at the 14 stations that represented by green circled numbers in Figure 4, were used in the analysis.

The fault parameters including the estimated parameters, M_0, and v_r, through SETP 1 are shown in Table 3.2, and the asperity pattern obtained by the STEP2 is shown in Figure 6(a). The asperity distribution obtained from this study is consistent with the result estimated by Aoi *et al*. (2007) shown in Figure 6 (b); large asperity concentrates on the upper part of the fault plane.

3.3. Comparison of Acceleration Envelope and Seismic Intensity

The validity of the estimated asperity pattern is discussed regarding the similarity of the acceleration envelopes. Figure 7 shows the examples of envelopes both for recorded and simulated acceleration time history. The recorded acceleration time history is converted to rock surface level with the shear wave velocity of 500m/sec. These acceleration envelopes are smoothed by the rectangular window of 1.5sec widths. As shown in Figure 7, these acceleration envelopes based on estimated asperity are different in detail from the recorded envelopes, however, the result shows better consistency than that based on the uniform asperity pattern (Figure 7 (a)). The concentration of aceleration power is reproduced in the case of asperity pattern-considered.

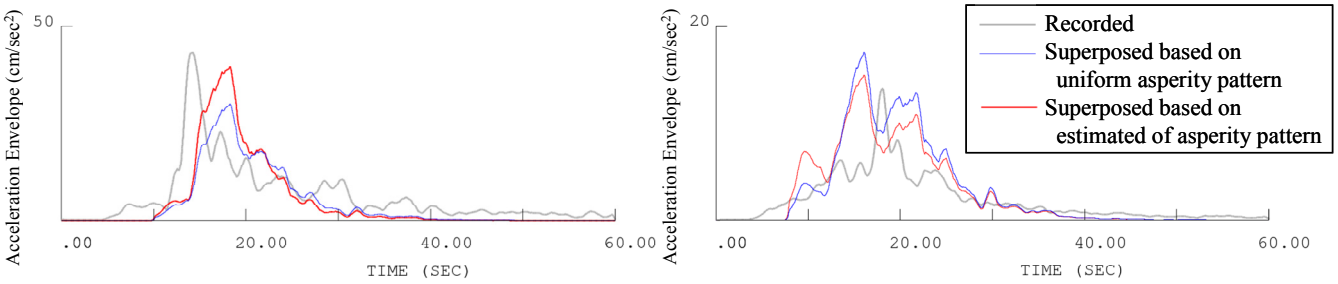

(a) ISKH01, NS (The Noto Hanto Earthquake in 2007)

(b) NIGH15, EW (The Niigataken Chuetsu-oki Earthquake in 2007)

Figure 7 Comparison of Envelope of Recorded and Simulated Acceleration Time Histories

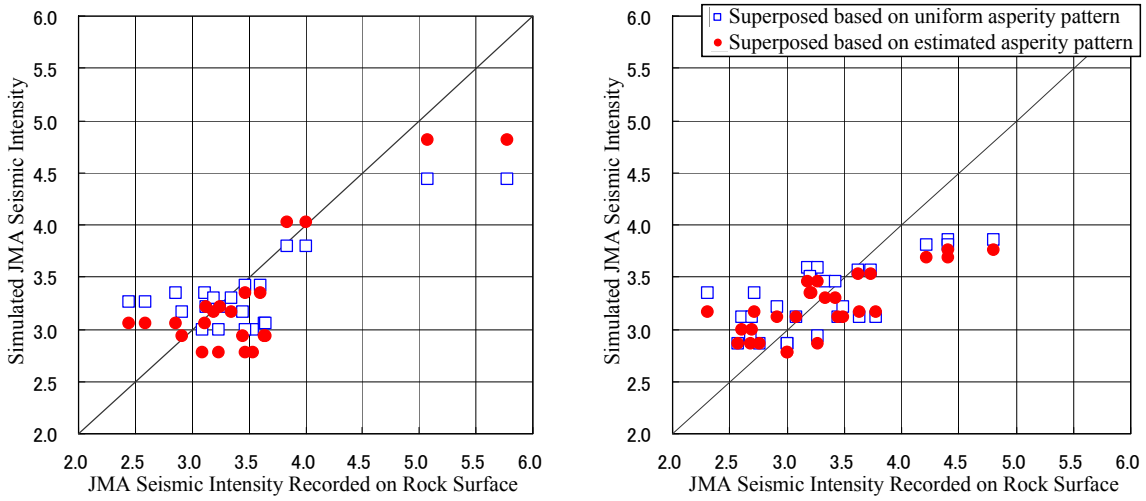

(a) The Noto Hanto Earthquake in 2007

(b) The Niigataken Chuetsu-oki Earthquake in 2007

Figure 8 Comparison of JMA Seismic Intensity on the Rock Surface

Figure 8 shows the comparison of JMA seismic intensity scale at the observation stations. The JMA seismic intensity scale is determined by use of three components of acceleration time histories processed with a specific band-pass filter prescribed by JMA. The estimation error of JMA seismic intensity is shown in Figure 8. As shown in Figure 8, the consideration of asperity distribution generally improves the accuracy of estimation of seismic intensity.

3.4. Discussion about the Area of Fault Plane and the Distribution of Asperity

In this section, the validity of the consideration of asperity pattern for strong motion simulation is discussed using the result for relatively large earthquake, the 2003 Tokachi-oki Earthquake. Figure 9 shows the asperity pattern of the 2003 Tokachi-oki Earthquake estimated by Kuse *et al*., (2005). The fault length and width are as L=140km and W=160km. As shown in Figure 9, there obtained three distinguished asperities on the fault.

Figure 10 shows the examples of acceleration envelopes both for recorded and simulated acceleration time history. As shown Figure 10, the duration is relatively long because of large fault, and the acceleration envelope has several peaks. It is also observed that time trend of acceleration envelop both for recorded and simulated are consistent.

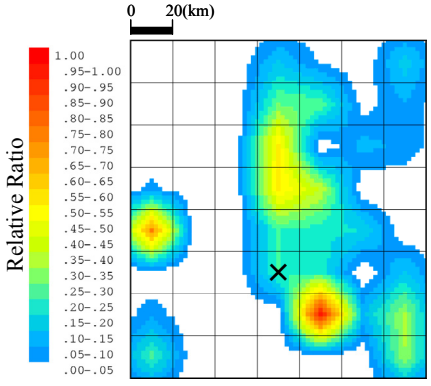

Figure 9 Distribution of Asperity (2003 Tokachi-oki Earthquake (Kuse *et al*., 2005))

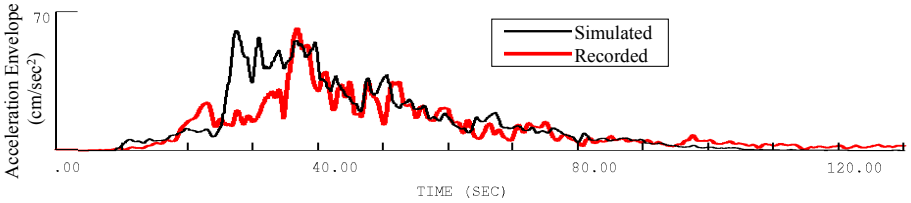

Figure 10 Comparison of Envelope of Recorded and Simulated Acceleration Time Histories (2003 Tokachi-oki Earthquake (Kuse *et al*., 2005), HDKH06, NS)

4. CONCLUSIONS

In this paper, the asperity distributions for the Noto Hanto Earthquake in 2007 and the Niigataken Chuetsu-oki Earthquake in 2007, were estimated by using the inversion technique developed by the authors. The major results derived here may be summarized as follows.

1. The dataset of strong motion records on rock surface for these two earthquakes has been obtained. The original acceleration records were obtained at underground bed rock level in KiK-net observation systems.
2. The asperity distributions were estimated by inversion technique developed by the authors. In the analysis, the acceleration envelope for the unit sub-event motion given by the strong motion prediction model, EMPR, was applied. The asperity pattern obtained in this study represents the relative ratio of release of acceleration power over the fault.
3. The rock surface motions were simulated for the observation points on the basis of the estimated asperity distribution by using the simulation technique, EMPR. The simulated rock surface motions were compared with observed motions in terms of the acceleration envelope and the JMA seismic intensity. The result demonstrated the validity of the inversion carried out in this study.
4. The case for large fault earthquake, the 2003 Tokachi-oki Earthquake, was introduced. It was shown that our inversion technique was valid regardless of the fault size.

REFERENCES

Aoi, S., Sekiguchi, H., Morikawa, N., Kunugi, K., and Shirasaka, M. (2007). Source Process of the 2007 Niigata-ken Chuetsu-oki Earthquake Derived from Near-fault Strong Motion Data. http://www.k-net.bosai.go.jp/k-net/topics/chuetsuoki20070716/inversion/ksw_ver070816_NIED_Inv_eng.pdf.

Aoi, S., and Sekiguchi, H. (2007). Source Process of the Noto Hanto Earthquake Derived from Near-fault Strong Motion Data. http://www.k-net.bosai.go.jp/k-net/topics/noto070325/ (in Japanese)

Enomoto, Y., Sugito, M., and Kuse, M. (2007). The Study of Earthquake Response Analysis based on the KiK-net Records. *JSCE-Chubu Annual Meeting*, I-20 (CD-ROM) (in Japanese)

Kuse, M., Sugito, M., Nojima, N., Yagyuu, K. (2004a). Inversion of Source Process in Consideration of Filtered-Acceleration Power Time Histories. *Journal of Structural Mechanics and Earthquake Engineering* **I-67: No, 759**, 409-414. (in Japanese)

Kuse, M., Sugito, M., and Nojima, N. (2004b). Inversion of Source Process in Consideration of Filtered-Acceleration Envelope, *13th World Conference on Earthquake Engineering*, Paper No.665. (CD-ROM)

Kuse, M., Sugito, M., and Nojima, N. (2005). Inversion of Asperity of the 2003 Tokachi-oki Earthquake of M8.0 and Estimation of Local Seismic Intensity Distribution, *Institute of Earthquake Engineering and Enginieering Seismology, Earthquake Engineering In The 21st Century, Ohrid, Macedonia*, Paper No.T2-15 (CD-ROM)

Midorikawa, S. (1987). Prediction of Isoseismal Map in the Kanto Plain due to Hypothetical Earthquake, *Journal of Structural Engineering*, **Vol.33B**, 43-48. (in Japanese)

Sugito, M. (1995). Frequency-dependent Equivalent Strain for Earthquake Response Analysis of soft Ground, *Proc. of IS-Tokyo, '95, The First International Conference on Earthquake Geotechnical Engineering*, 655-660.

Sugito, M., Furumoto, Y., and Sugiyama, T. (2000). Strong Motion Prediction on Rock Surface by Superposed Evolutionary Spectra. *12th World Conference on Earthquake Engineering*, Paper No.2111. (CD-ROM)